Supplemental Figures

Figure S1

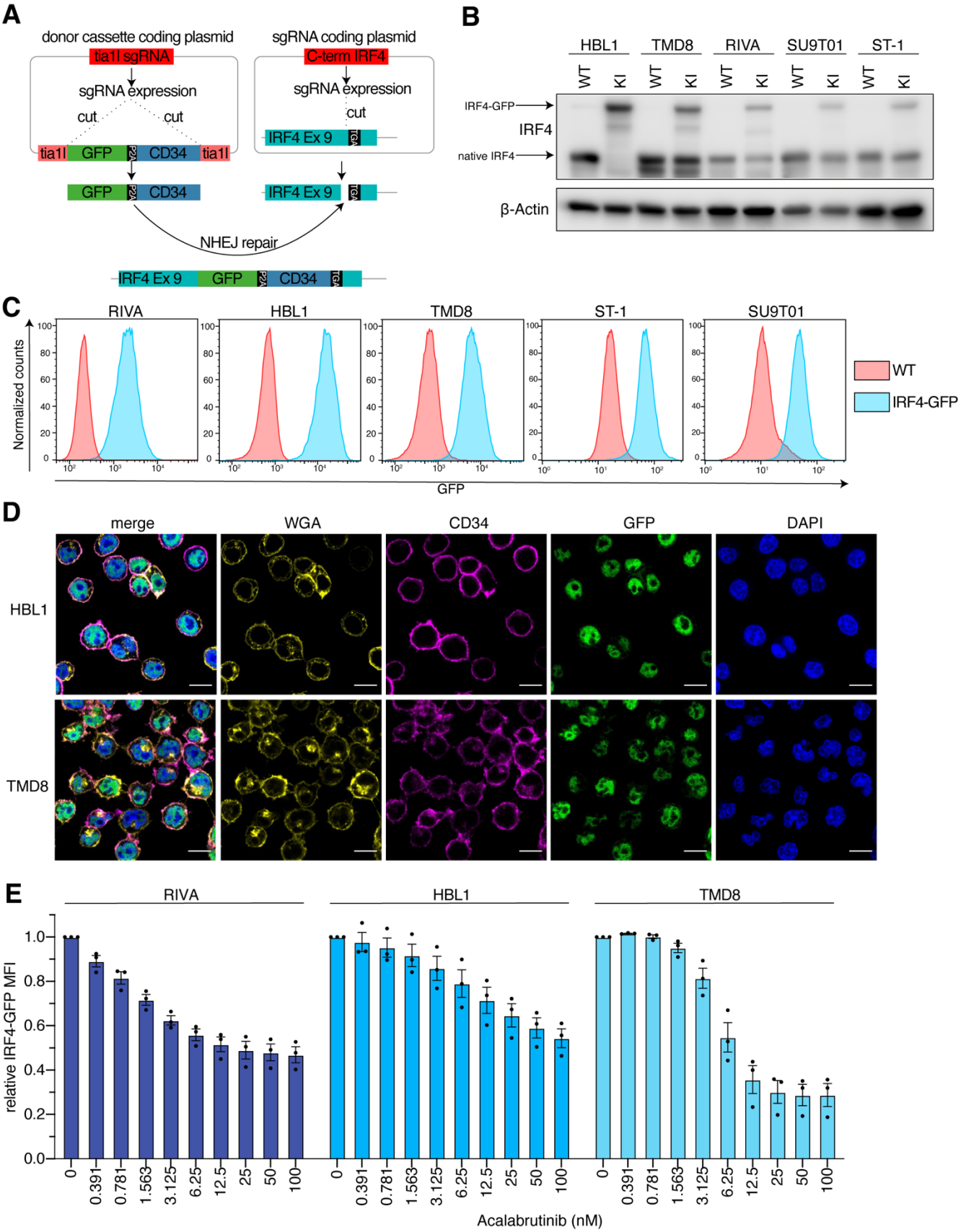

Supplemental Figure 1. IRF4-GFP knock-in reporter cell lines.

A. Scheme of two plasmid knock-in system exploiting non-homologous end joining (NHEJ) repair mechanisms. A donor plasmid carrying a GFP-P2A-CD23 cassette and a sgRNA plasmid leading the Cas9 protein to cut at the C-terminus of IRF4 were brought into the cells by electroporation and genomic double strand break is repaired by NHEJ inserting the donor cassette. **B.** Immunoblot validations of wildtype (WT) and IRF4-knock-in (KI) cells in the indicated cell lines using indicated antibodies. Lower IRF4 band represents the native IRF4 protein and upper band the IRF4-GFP fusion protein. **C.** FACS histograms displaying the FL1/GFP channel of wildtype (WT, red) and IRF4-GFP (blue) knock-in cell lines as indicated. **D.** Confocal microscopy in HBL1 and TMD8 cells. Wheat-germ agglutinin-Alexa 647 stain in yellow, CD34-PE stain in magenta, IRF4-GFP fluorescence in green and DAPI in blue. **E.** Mean IRF4-GFP fluorescence intensity in RIVA, HBL1 and TMD8 cells treated with the indicated concentrations of acalabrutinib. Error bars represent SEM of three independent experiments.

Figure S2

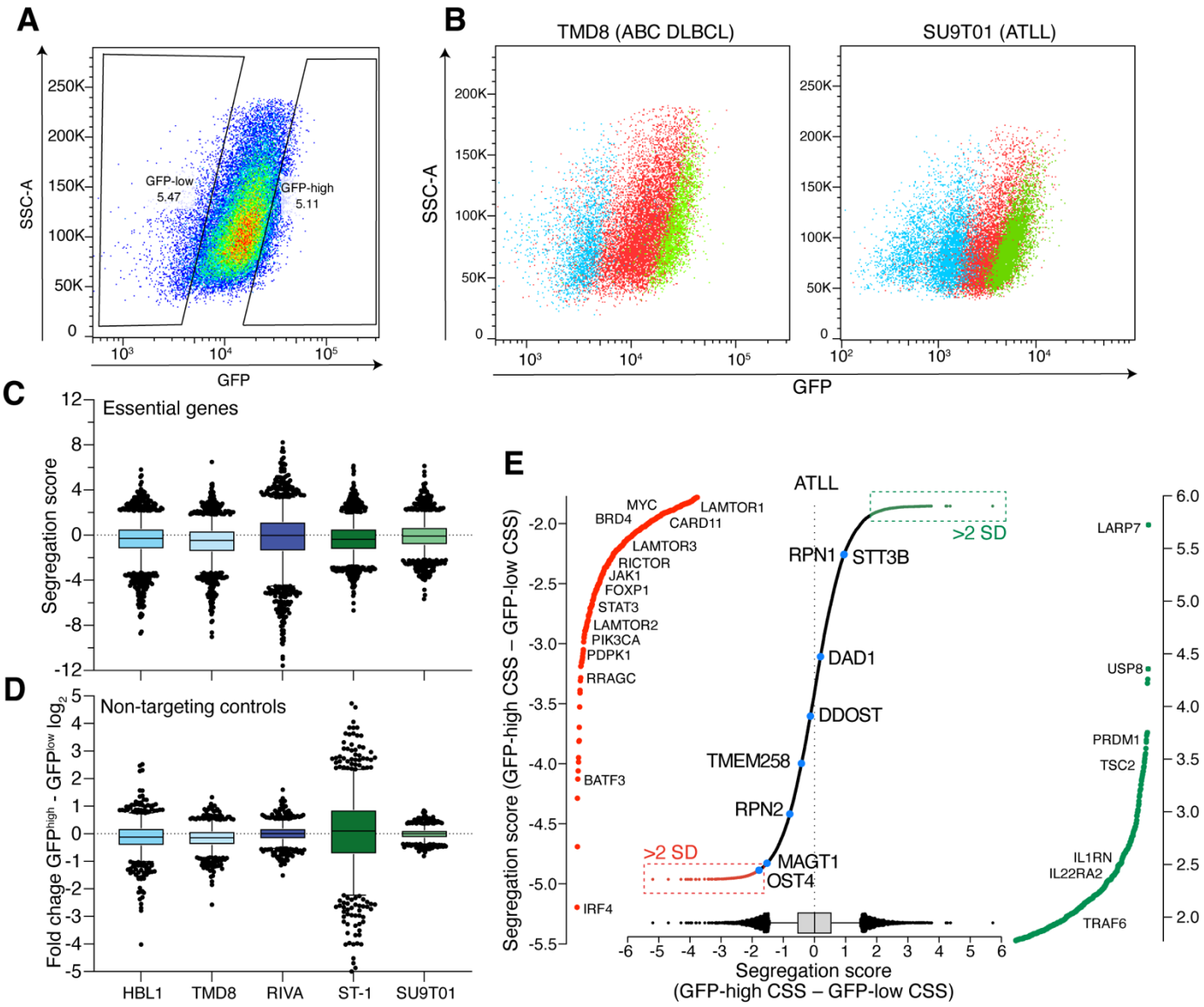

Supplemental Figure 2. IRF4-GFP CRISPR screen in adult T-cell lymphoma and screen controls.

A. FACS gating strategy for IRF4-GFP CRISPR screens sorting the top and bottom 5% population. **B.** Post-sort FACS analysis of TMD8 and SU9T01 cells. Red populations represent the unsorted, blue population the bottom 5% sorted (IRF4-GFP low) and green the top 5% sorted (IRF4-GFP high) population. **C.** Segregation score of common essential genes (defined by DepMap) in IRF4-GFP CRISPR screens in three ABC DLBCL cell lines (HBL1, TMD8 and RIVA) and two adult T-cell lymphoma cell lines (ST-1, SU9T01). **D**. Fold change of non-targeting control sgRNAs (GFP^{high} minus GFP^{low}) in IRF4-GFP CRISPR screens in three ABC DLBCL cell lines (HBL1, TMD8 and RIVA) and two adult T-cell lymphoma cell lines (ST-1, SU9T01). **E.** Ranked list of genes by their segregation score (CSS GFP^{high} – CSS GFP^{low}) with their 5-95% percentile (box and whiskers) averaged from two

adult T-cell lymphoma cell lines (ST-1, SU9T01). Outliers >2 SD with negative segregations scores are highlighted in red, subunits of the OST complex in blue and outliers >2 SD with positive segregation scores in green.

Figure S3

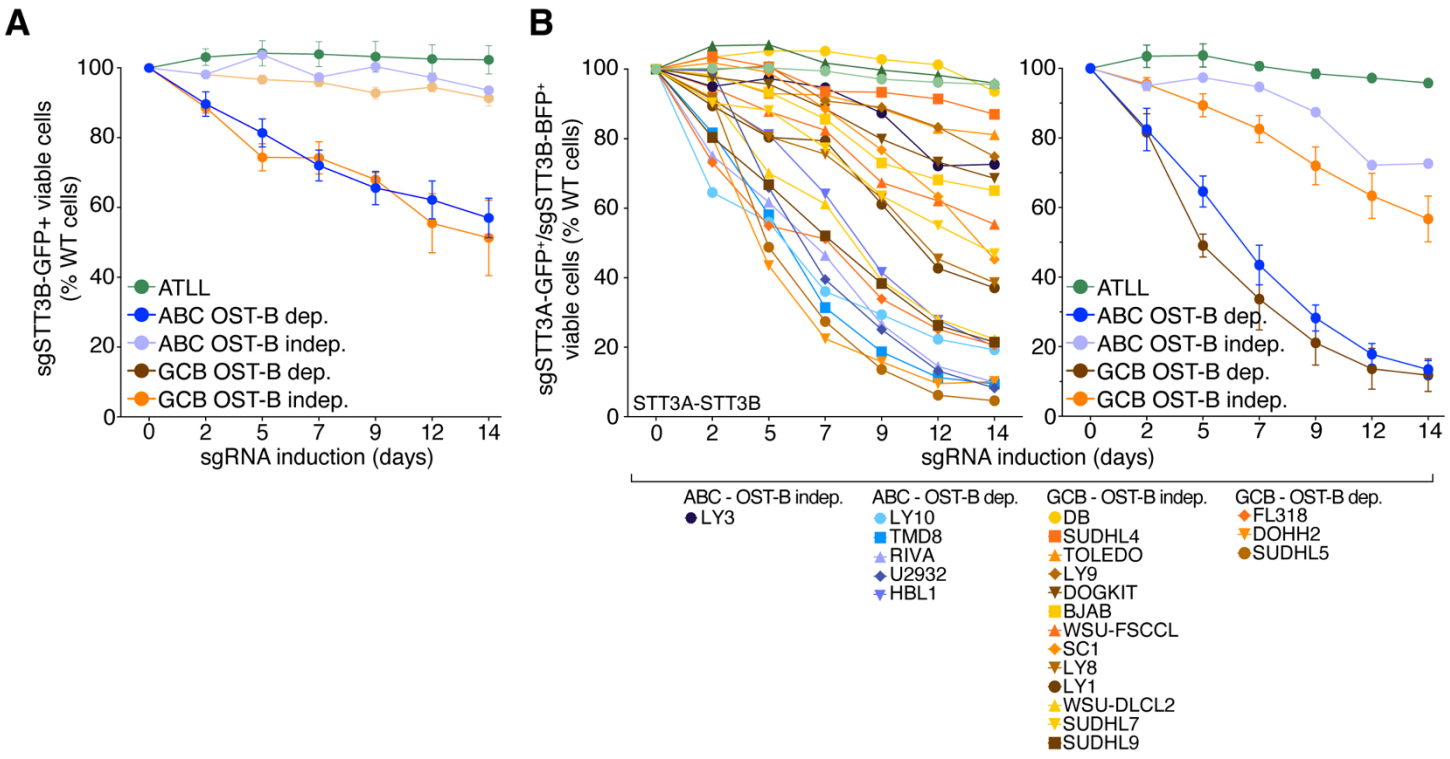

Supplemental Figure 3. The OST is essential for DLBCL.

A. Toxicity of STT3B knockout in OST-dependent/independent ABC and GCB lines and in adult T-cell leukemia/lymphoma (ATLL) lines. Viable cell numbers are normalized to day 0. Error bars represent SEM. dep.: dependent; indep.: independent. **B.** Toxicity of sgRNAs targeting both STT3A and STT3B (double knockout) normalized to day 0 (day of sgRNA induction). Left, toxicity of individual cell lines colored by their lymphoma subtype (ATLL, adult T-cell lymphoma, green, ABC DLBCL lines, blue, or GCB DLBCL lines, orange/yellow/brown). Mean of three biologically independent experiments. Right, toxicity grouped by genetic dependency of the OST-B complex (STT3B knockout).

Figure S4

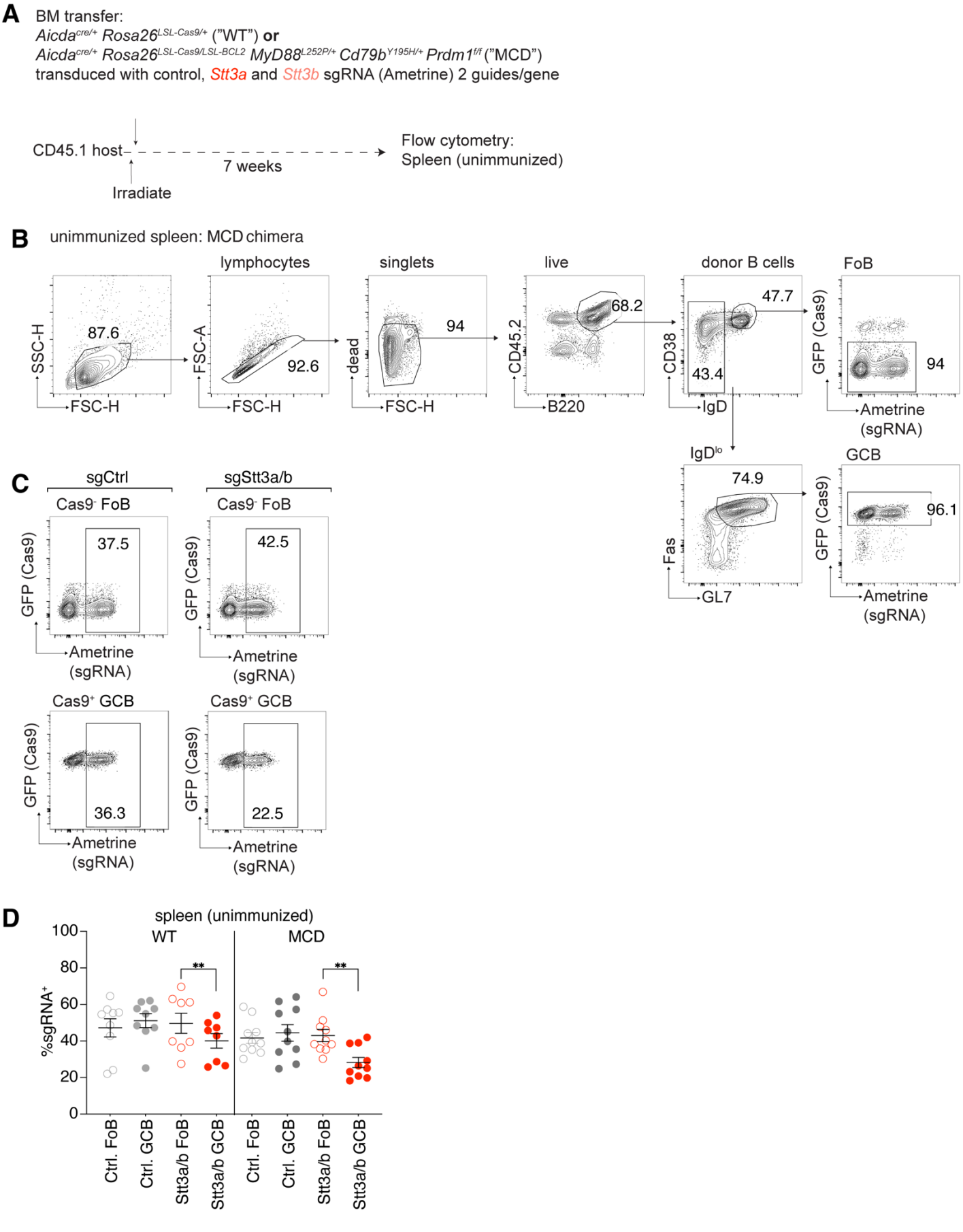
A
BM transfer:
Aicda cre/+ Rosa26 LSL-Cas9/+ ("WT") or
Aicda cre/+ Rosa26 LSL-Cas9/LSL-BCL2 MyD88 L252P/+ Cd79b Y195H/+ Prdm1 f/f ("MCD")
transduced with control, Stt3a and Stt3b sgRNA (Ametrine) 2 guides/gene
CD45.1 host
Irradiate
7 weeks
Flow cytometry:
Spleen (unimmunized)
B
unimmunized spleen: MCD chimera
lymphocytes
singlets
live
donor B cells
FoB
SSC-H
FSC-H
87.6
FSC-A
92.6
dead
94
CD45.2
B220
68.2
CD38
IgD
47.7
43.4
GFP (Cas9)
Ametrine (sgRNA)
IgDlo
74.9
Fas
GL7
GCB
96.1
C
sgCtrl
sgStt3a/b
Cas9- FoB
37.5
42.5
Cas9+ GCB
36.3
22.5
D
spleen (unimmunized)
WT
MCD
%sgRNA+
100
80
60
40
20
0
**
Ctrl. FoB
Ctrl. GCB
Stt3a/b FoB
Stt3a/b GCB

Supplemental Figure 4. The role of the OST complex in radiation chimeras.

A. Experimental scheme for wildtype (WT) chimeras oder chimeras modeling the MCD DLBCL subtype **B.** Gating scheme to follicular B cells (FoB) or germinal center B cells (GCB) in an unimmunized spleen from an MCD radiation chimera. **C.** Percentages of Stt3a/b sgRNA positive GCBs to Stt3a/b sgRNA positive FoB in MCD radiation chimeras in unimmunized spleen generated as in panel A. **D.** Percentages of frequency Stt3a/b sgRNA positive GCBs to Stt3a/b sgRNA positive FoB in wildtype (WT) radiation chimeras or MCD radiation chimeras in unimmunized spleen as generated in panel A. Data are pooled from 2 independent experiments representative of 4 with 5 mice per group. **P ≤ 0.01 (unpaired two-tailed t test).

Figure S5

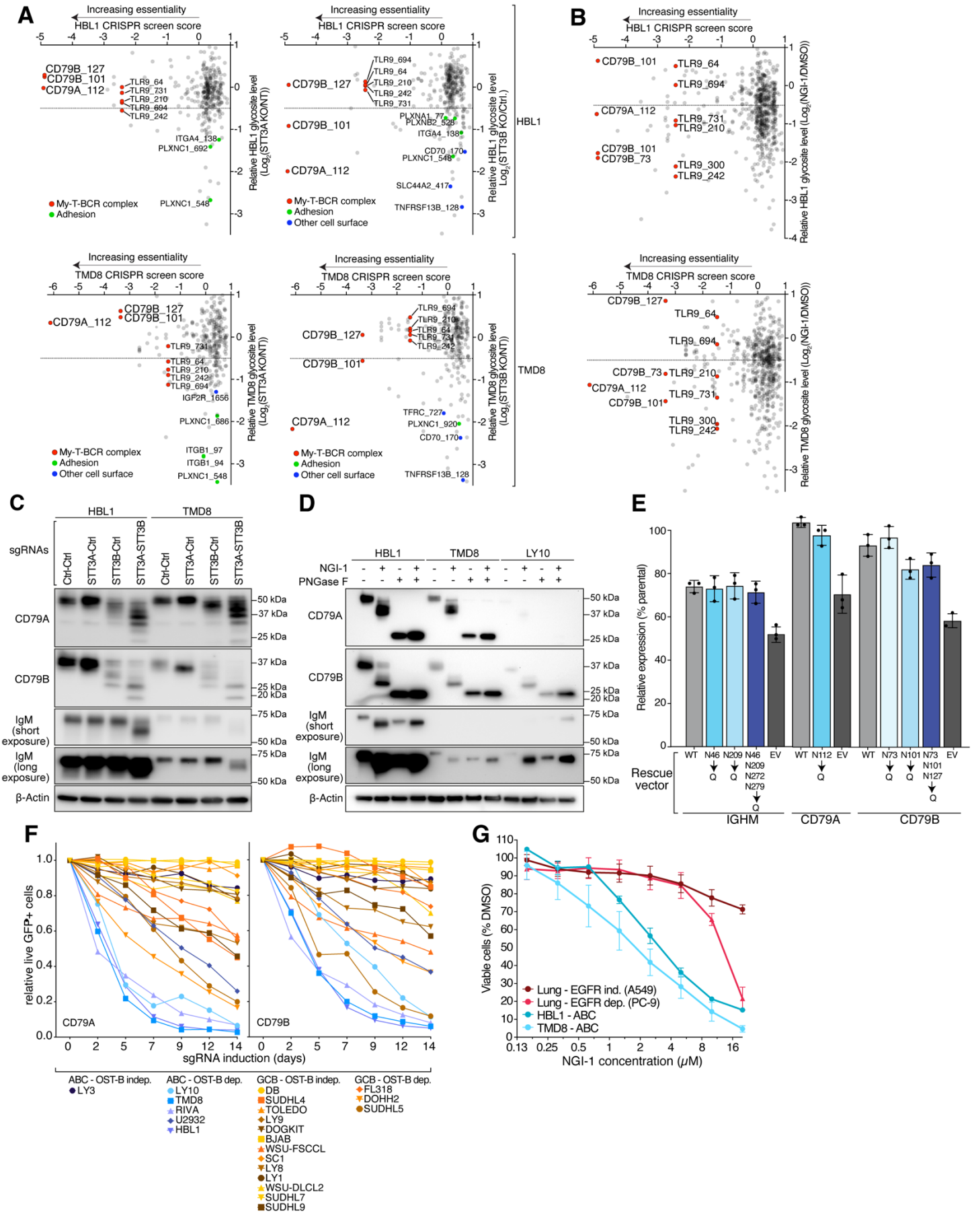
A
Increasing essentiality
HBL1 CRISPR screen score
CD79B_127
CD79B_101
CD79A_112
TLR9_64
TLR9_731
TLR9_210
TLR9_694
TLR9_242
ITGA4_138
PLXNC1_692
PLXNC1_548
My-T-BCR complex
Adhesion
Relative HBL1 glycosite level (Log2(STT3A KO/NT))
Relative HBL1 glycosite level Log2(STT3B KO/Ctrl.)
Other cell surface
PLXNA1_77
PLXNB2_928
CD70_170
SLC44A2_417
TNFRSF13B_128
HBL1
B
Relative HBL1 glycosite level (Log2(NGI-1/DMSO))
CD79B_101
CD79B_73
TLR9_64
TLR9_694
TLR9_731
TLR9_210
TLR9_300
TLR9_242
TMD8 CRISPR screen score
Relative TMD8 glycosite level (Log2(STT3A KO/NT))
Relative TMD8 glycosite level (Log2(STT3B KO/NT))
IGF2R_1656
PLXNC1_686
ITGB1_97
ITGB1_94
TFRC_727
PLXNC1_920
TMD8
Relative TMD8 glycosite level (Log2(NGI-1/DMSO))
C
HBL1
TMD8
sgRNAs
Ctrl-Ctrl
STT3A-Ctrl
STT3B-Ctrl
STT3A-STT3B
CD79A
CD79B
IgM (short exposure)
IgM (long exposure)
β-Actin
50 kDa
37 kDa
25 kDa
20 kDa
75 kDa
D
LY10
NGI-1
PNGase F
E
Relative expression (% parental)
WT
N46
N209
N46 N209 N272 N279
EV
N112
N73
N101
N73 N101 N127
Rescue vector
IGHM
CD79A
CD79B
F
relative live GFP+ cells
sgRNA induction (days)
ABC - OST-B indep.
LY3
ABC - OST-B dep.
LY10
TMD8
RIVA
U2932
HBL1
GCB - OST-B indep.
DB
SUDHL4
TOLEDO
LY9
DOGKIT
BJAB
WSU-FSCCL
SC1
LY8
LY1
WSU-DLCL2
SUDHL7
SUDHL9
GCB - OST-B dep.
FL318
DOHH2
SUDHL5
G
Viable cells (% DMSO)
Lung - EGFR ind. (A549)
Lung - EGFR dep. (PC-9)
HBL1 - ABC
TMD8 - ABC
NGI-1 concentration (μM)

Supplemental Figure 5. The B-cell receptor is glycosylated by the OST complex.

A. The essential glycoproteome of HBL1 (upper two panels) or TMD8 (lower two panels) cells. The CRISPR screen score (essentiality score) of the respective cell line (x-axis) is plotted by the glycosite log_2 fold changes after genetic deletion of either STT3A (left two panels) or STT3B (right two panels) of the same cell line. Each dot represents an individual glycosite. My-T-BCR related proteins are called out in red, adhesion related proteins in green and other cell surface proteins in blue. **B.** The essential glycoproteome of HBL1 (upper panels) or TMD8 (lower panels) cells. The CRISPR screen score (essentiality score) of the respective cell line (x-axis) is plotted by the glycosite log_2 fold changes after 48h treatment with NGI-1 of the same cell line. **C.** Immunoblots of CD79A, CD79B and IgM in HBL1 or TMD8 cells with knockout of STT3A, STT3B or STT3A/B double knockout. **D.** Immunoblots of the BCR complex (CD79A, CD79B, IgM) as indicated in HBL1, TMD8, RIVA and OCI-Ly10 cells treated for 24h with NGI-1 and/or treated in vitro with PNGase F as indicated. **E.** Relative cell surface expression of the indicated rescue vectors expressed in TMD8 cells after knockout of endogenous IgM, CD9A or CD79B expression. Mean of three independent replicates (± SEM). ns, non-significant, ***P ≤ 0.001 (one-way ANOVA) compared to wildtype. **F.** Toxicity of sgRNAs targeting CD79A (left panel) or CD79B (right panel) in the indicated cell lines normalized to day 0 (day of sgRNA induction). **G.** MTS proliferation assays in TMD8, HBL1, A549 (lung adenocarcinoma EGFR independent) and PC-9 (lung adenocarcinoma EGFR dependent) treated with NGI-1 normalized to DMSO treated control cells. Error bars represent SEM, data from at least three independent replicates.

Figure S6

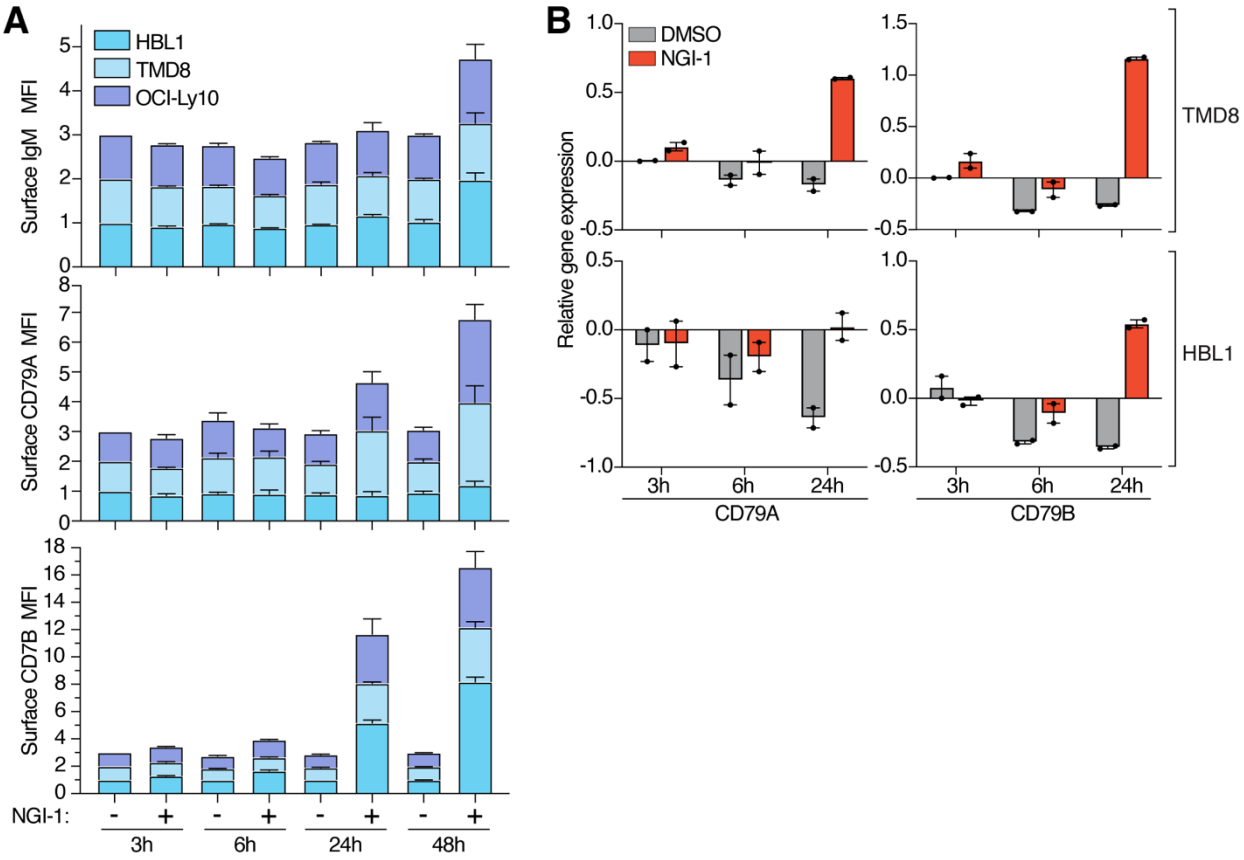

Supplemental Figure 6. B-cell receptor deglycosylation leads to higher surface expression. **A.** Cumulative cell surface expression of the BCR complex (IgM, CD79A and CD79B) in HBL1, TMD8 and OCI-Ly10 cells assessed by flow cytometry after NGI-1 treatment for the indicated times. Error bars represent SEM. Data from three independent replicates. **B.** Digital gene expression (RNAseq) normalized $\log_2$ fold changes of CD79A and CD79B at the indicated timepoints in HBL1 and TMD8 cells treated with DMSO (grey) or NGI-1 (red). Mean of two independent replicates.

Figure S7

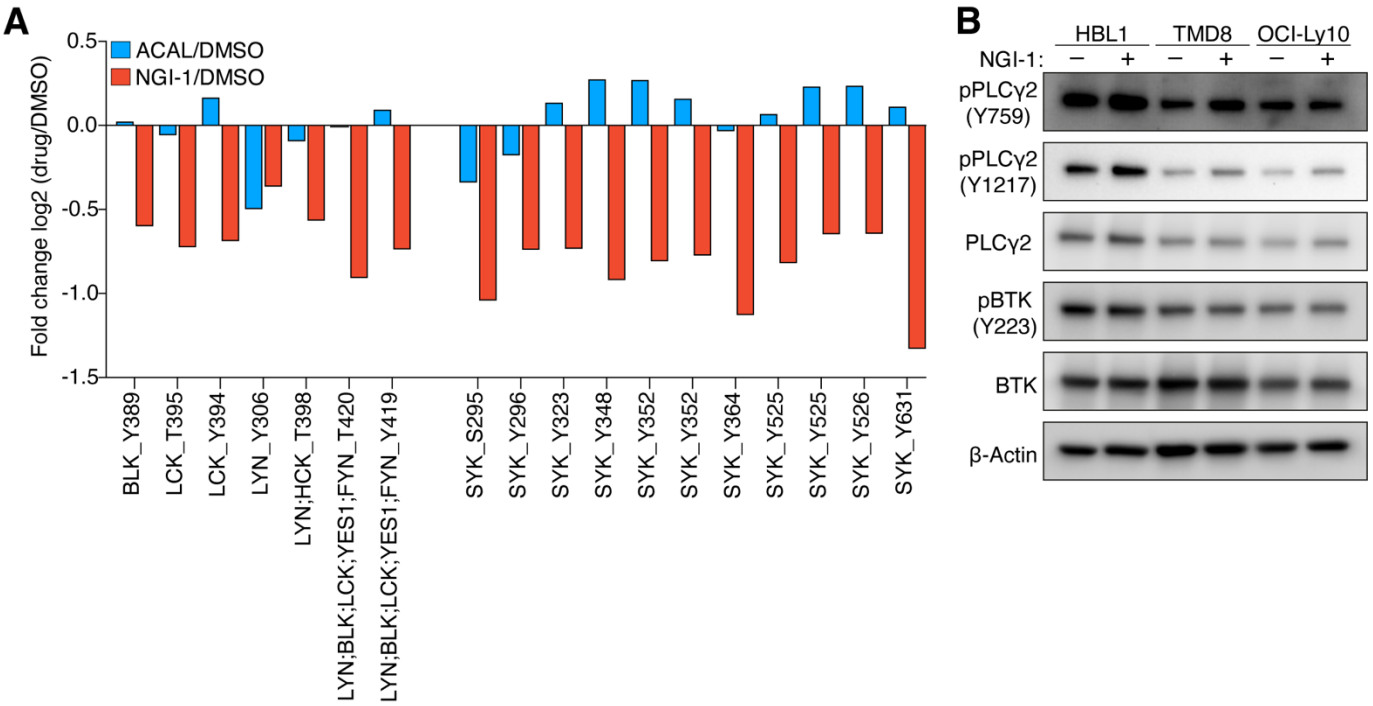

Supplemental Figure 7. B-cell receptor deglycosylation leads to signaling changes in proximal BCR signaling components.

A. Average (HBL1 and TMD8) changes of phosphorylation after 16h treatment with acalabrutinib (ACAL, blue) or NGI-1 (red) in proximal BCR signaling members by global phosphotyrosine proteomics (pYome). **B.** Immunoblots using the indicated antibodies in HBL1, TMD8 and OCI-Ly10 cells treated with NGI-1 for 16h.

Figure S8

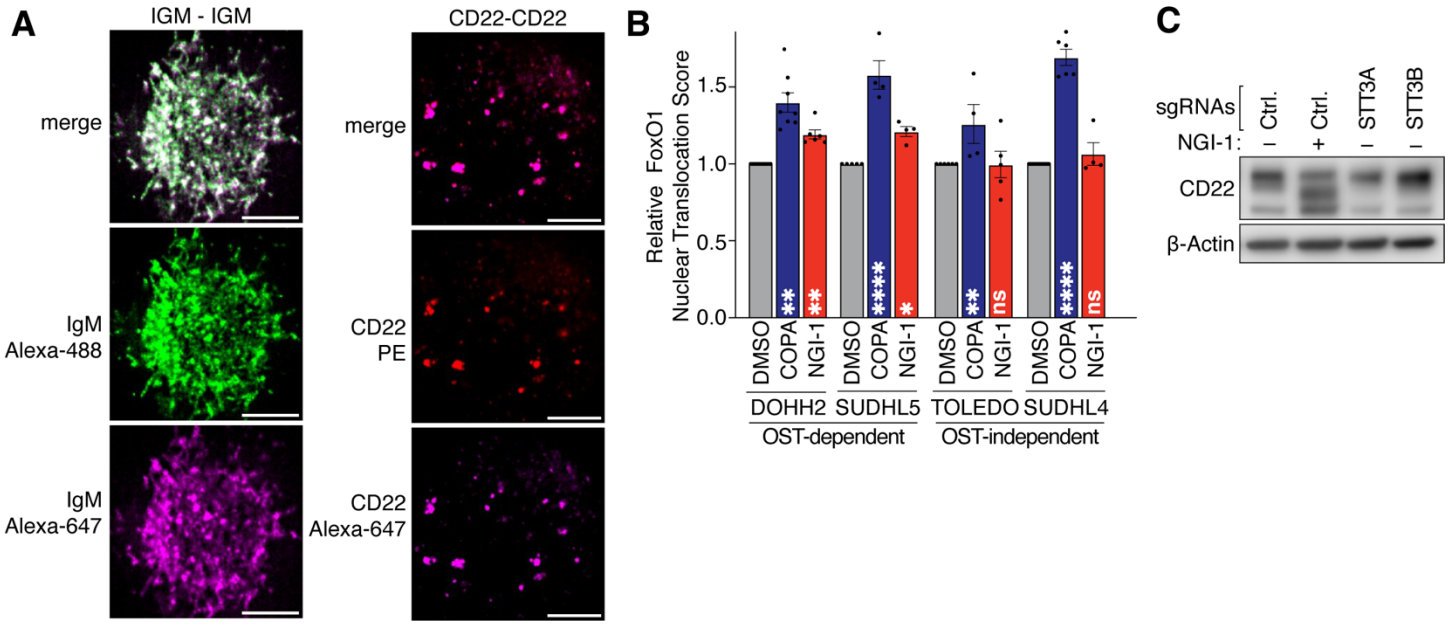

Supplemental Figure 8. BCR deglycosylation leads to recruitment of CD22 on the cell surface to the BCR and signaling alterations in GCB DLBCL.

A. Dual color iSIM images of TMD8 cells stained for IgM or CD22 with the indicated antibodies. Scale bar is 5μm. **B.** Relative FoxO1 nuclear translocation score assessed by imaging flow cytometry (ImageStream) in DOHH2, SUDHL5 (both OST dependent), TOLEDO or SUDHL4 (both OST independent) cells treated for 6h with 50nM copanlisib or 16h with 5μM NGI-1 as indicated normalized to each DMSO treatment. Error bars represent SEM of at least three independent experiments. *P ≤ 0.05, **P ≤ 0.01, ****P ≤ 0.0001 (one-way ANOVA). Ns, non-significant. **C.** Immunoblots using the indicated antibodies in TMD8 cells transduced with control sgRNA or sgRNAs targeting either STT3A or STT3B as indicated and treated with NGI-1 as indicated for 16h.

Figure S9

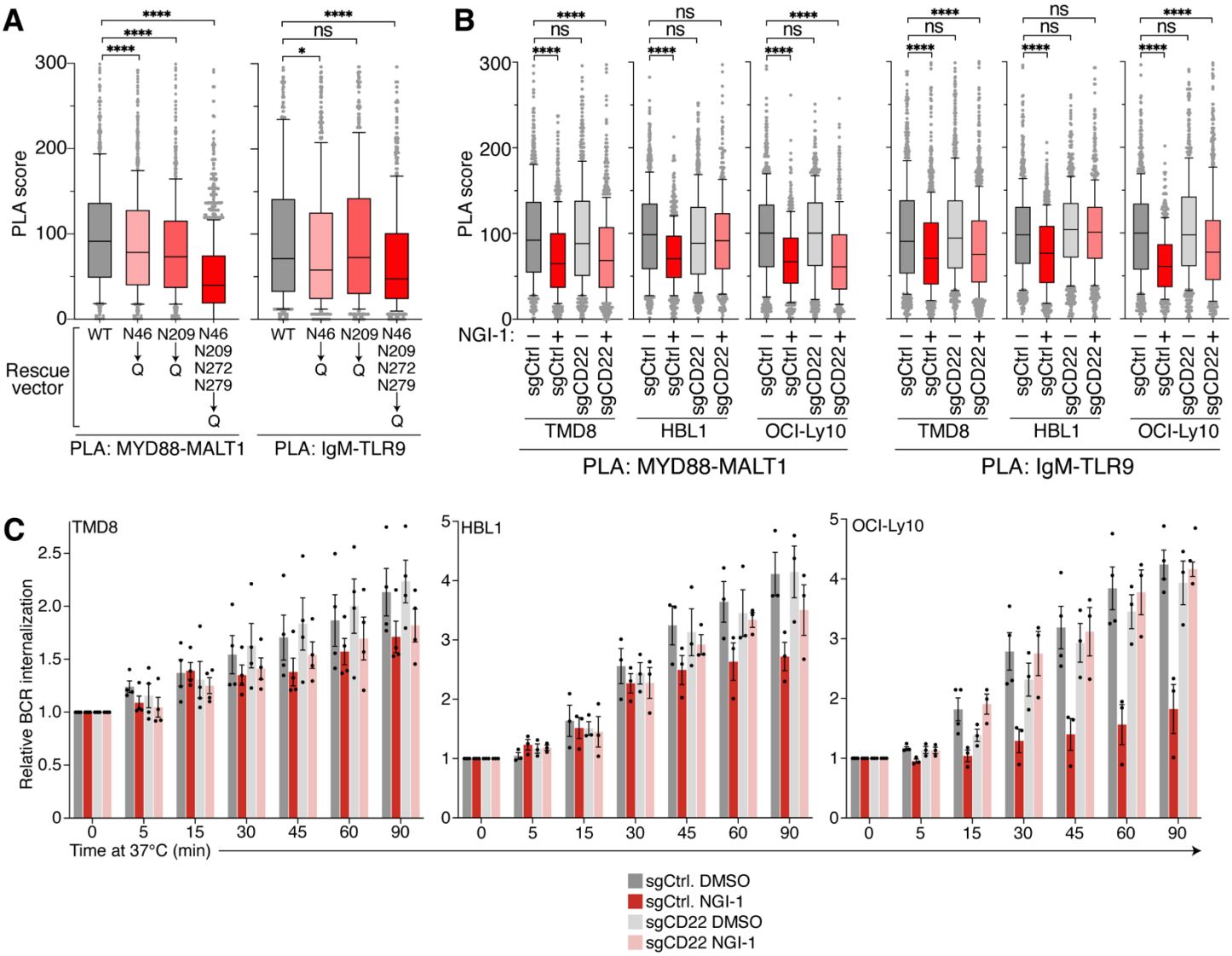

Supplemental Figure 9. BCR internalization and My-T-BCR formation in glycosylation deficient cells.

A. PLA scores of the MYD88-MALT1 PLA (left) or IgM-TLR9 PLA (right) in TMD8 IgM asparagine mutant isoforms as indicated after knockout of endogenous IgM. Box and whiskers: 10-90% percentile. Ns, non-significant, *P ≤ 0.05, ****P ≤ 0.0001 (one-way ANOVA). **B.** PLA scores of the MYD88-MALT1 PLA (left) or IgM-TLR9 PLA (right) in TMD8, HBL1 or OCI-Ly10 cells transduced with control sgRNA or sgRNAs targeting either STT3A or STT3B as indicated and treated with NGI-1 as indicated for 16h.Box and whiskers: 10-90% percentile. Ns, non-significant,****P ≤ 0.0001 (one-way ANOVA). **C.** Mean (± SEM) relative BCR internalization over 90 mins at 37°C in TMD8 (left panel) or OCI-Ly10 cells (right panel) transduced with control (Ctrl.) sgRNA or sgRNA targeting CD22 treated with NGI-1 for 24h as indicated. ****P ≤ 0.0001 (one-way ANOVA). Error bars represent SEM of at least three independent experiments.

Figure S10

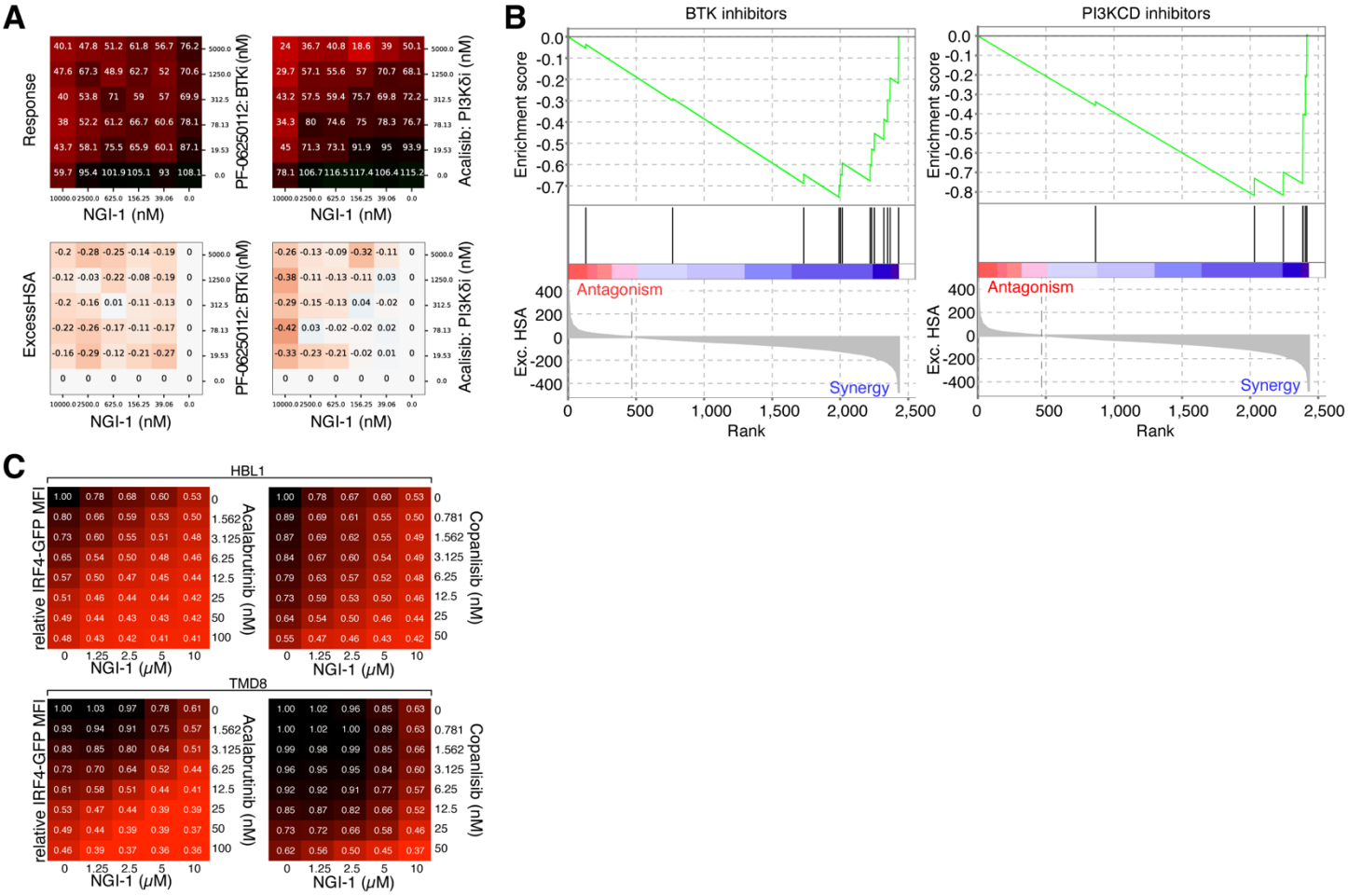

Supplemental Figure 10. NGI-1 synergizes with BTK and PI3K inhibitors.

A. Response matrices (upper panels) and Excess HSA matrices (lower panels) for NGI-1 vs. the BTK inhibitor PF-06250112 (left panel) and the PI3K inhibitor Acalisib (right panel) in TMD8 cells in 6x6 blocks using high throughput combinatorial drug screens (MIPE 5.0). **B.** BTK inhibitor (left) and PI3K inhibitor (rights) “drug set enrichment analysis” plots in combinatorial high throughput drug screens with NGI-1. **C.** IRF4-GFP MFI (IRF4-GFP knock-in reporter) of HBL1 cells (upper panel) and TMD8 cells (lower panel treated with indicated doses of NGI-1 and acalabrutinib (left panels) or copanlisib (right panels). Values represent MFI of at least three independent experiments.